PAPER P

ESTIMATION OF STATISTICAL PROPERTIES IN RANDOM MEDIA USING DIFFRACTION TOMOGRAPHY

Guan Y. Wang, Jerry M. Harris and Jesse C. Costa

ABSTRACT

The basic problem of the inverse scattering is to determine unknown material properties by analyzing the scattering of a wave propagating through the material. When the distribution of the small scale inhomogeneities is too complicated to describe deterministically, we may treat the medium as random. By probing the random medium with multiple sources and receivers, the second order statistics of the medium can be inferred from the power spectrum of the scattered field. The resolved statistical quantiles may be used to identify, for example, fracture scales and orientations, or to facilitate other reservoir simulation modalities.

INTRODUCTION

Waves in random media are often described using the diffusion equation. Beyond traditional approach of diffusion, we examine the amplitude-amplitude correlations using the full wave (scalar or vector) representations. In synthetic simulations created with the Born approximation or finite difference, the random distribution is characterized by ellipsoidal autocorrelation functions. We assume the large scale component of the elastic parameters is constant and the perturbations are random functions of spatial variables. We want to determine the correlation function of the inhomogeneities from the measured data.

The spatial power spectra of the scattered fields are utilized to characterize patterns of inhomogeneities. Without confusion, we use power spectrum for spatial power

spectrum for short. By probing the random medium with multiple sources and receivers, the second order statistics of the medium can be inferred from the power spectrum of the scattered field by extending diffraction tomographic procedure. The resolved statistical quantities may be used to identify fracture scales and orientations, or can be directly used in reservoir integrating study.

CHARACTERIZATION OF RANDOM MEDIA

Let $m_i(\mathbf{x}), i = 1, 2, 3$ be a random isotropic elastic medium, where $\mathbf{x} = (x, z)$, which may consist of p-wave velocity, v_p/v_s ratio and density. The function $m_i(\mathbf{x})$ can be decomposed into $m(\mathbf{x}) = m^0 + m'(\mathbf{x})$, where m^0 represent the large scale inhomogeneities while $m'(\mathbf{x})$ represents small scale inhomogeneities. Only second-order statistics are considered since the most likely statistical characteristics of $m(\mathbf{x})$ that can be recovered from seismic data are their first two moments, i.e., mean value m^0 and autocorrelation function $c_i(\mathbf{x}_1, \mathbf{x}_2) =< m_i(\mathbf{x}_1)m_i(\mathbf{x}_2) >$. The correlation between the elastic parameters is still an open question and beyond the scope of this paper. We assume the cross-correlations between the three parameters $m_i(\mathbf{x})$ are independent.

The scattering properties of the medium depend not only on the mean of m^0 but also on the autocorrelation function of the randomly varying part of the material property. The autocorrelation of the fluctuation is a measure of the size and shape of a typical irregularity in the medium. The correlation function $c_i(\mathbf{x}_1, \mathbf{x}_2)$ is well understood if $m(\mathbf{x})$ is a random function of time, such as the density of the atmosphere when temperature fluctuates. In that case, ensemble average may be taken. This is a general way of characterizing a random variable by means of averages, which in principle must be performed by repeating the experiment many times on different samples. This tacitly consideration is called the ergodic assumption. It is worth to notice that these averages may or may not have a direct connection with particular quantities that are found in a particular sample. In practice, we replace the ensemble average by the temporal average so long as the process is statistically stationary and the total amount of time large enough then all members of the ensemble will be encounter.

In a solid medium, however, the fluctuation of the property $m'(\mathbf{x})$ is not a function of the times at least for the durations of seismic experiments. By analogy to the ergodic assumption for temporal stochastic process, the ensemble average of the spatial random functions is approximated as the average over the volume, assuming that the fluctuation $m'(\mathbf{x})$ has spatial invariant statistical properties within the volume considered (Harris, 1994).

It can be shown that the ensemble average of the power spectrum is the average correlation function over the considered volume (Papoulis, 1965). Under these assumptions, correlation is spatial invariant, i.e., $c_i(\mathbf{x}_1, \mathbf{x}_2) = c_i(\mathbf{x}_1 - \mathbf{x}_2)$.

The correlation function can have various functional forms depending on the nature of the irregular medium such as the Gaussian form, the exponential form, and fractal form etc.. The form of the probability distributions governing $m_i(\mathbf{x})$ and the form of the correlation function are quite independent to each other. A function $m_i(\mathbf{x})$ obeying non-Gaussian statics may or may not have a Gaussian correlation function, and vice versa. Assuming the random function $m_i(\mathbf{x})$ has an exponential autocorrelation function (Ikelle, 1993)

$$c_i(\xi, \eta) = exp(-\sqrt{\frac{\xi^2}{a^2} + \frac{\eta^2}{b^2}}), \tag{1.1}$$

where a and b are the autocorrelation length scales. The spectrum of the media in the Fourier transform domain is constructed as

$$M_i(k_x, k_z) = |C_i(k_x, k_z)| exp(i\theta(k_x, k_z)), \tag{1.2}$$

where the uniform distribution $\theta \subset [0, 2\pi]$ is defined as the phase of the spectrum M_i. The random function m_i is then generated via inverse Fourier transform, i.e.

$$m_i(x, z) = FT_{2d}\{M_i(k_x, k_z) w(k_x, k_z)\}, \tag{1.3}$$

which has the desired autocorrelation function. Notice that the filter $w(k_x, k_z)$ is design to remove the D.C. component.

With Figure (1.1), we show the exponential autocorrelation functions of various

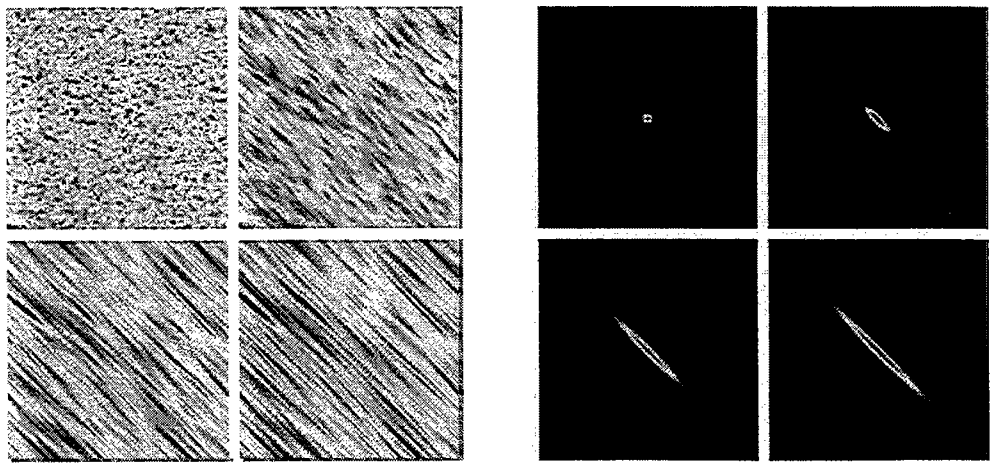

Figure 1.1: The left panel is the correlation functions with different vertical and horizontal correlation length a's and b's. The right panel is the realizations generated with the correlation functions.

correlation length. The realizations is intend to describe the inhomogeneities of the medium as isotropic or elongated in a specified direction.

THE SCATTERED FIELD AS A RANDOM VARIABLE

As said above, the detailed information about medium is not generally accessible by actual experiment and if not always meaningful. It is useful to consider the statistical behavior of the medium as a whole. Thus one has to manipulate the expressions for the deterministic scattered field in order to obtain quantities that can be related to the statistical quantities, namely, to replace the ensemble averages with spatial averages. The procedure which one has to employ when comparing the theory with results of the experiment, is obviously not very general.

The basic quantity needed in order to obtain information on the scattering medium is the distribution of the scattered intensity as a function of the scattering angle and the frequency. Under the hypothesis of stationarity, the autocorrelation function $< \hat{u}(r)\hat{u}(r+r') >$ depends only on the difference $(r+r') - r = r'$, where r' is correlation length.

In Figure (1.2) we indicate the average wavelength λ and the correlation length

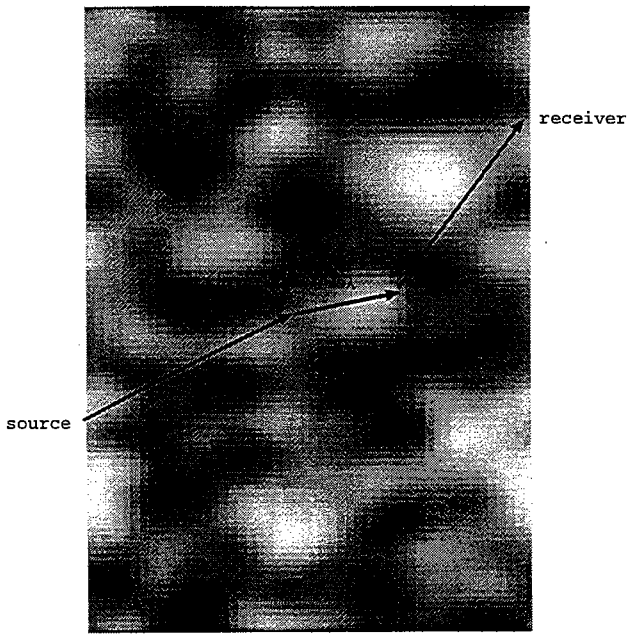

Figure 1.2: The random spatial distribution function $m_i(\mathbf{x})$. The weak scattering can be interpreted as $r_0 >> \lambda$, where λ is the average wavelength of the incident wave in the medium and r_0 is the aspect ratio $r_0 = a/b$.

r_0 of the fluctuations of elastic parameters. $r_0 = a/b$ is defined as the aspect ratio. The weak scattering can be interpreted as $\lambda >> r_0$ which is used to gauge the wave field modeling.

ESTIMATE CORRELATION FUNCTION OF MEDIA

We assuming the large scale component of the elastic parameters is constant and the perturbations are random functions of spatial variables with zero mean. We consider the inverse problems of determine the two-point spatial correlation function of the perturbation functions with the measured fluctuations of the scattered fields and their spatial correlations.

For the assumed statistical homogeneous medium, the correlation function depends only on the coordinate differences $r = r_2 - r_1$, i.e., $N_{12} = N_{12}(r)$. For $r = 0$, the function N_{12} achieves its maximum N_{11} , equal to the mean square fluctuations.

The correlation coefficient N is defined as the ratio of the correlation function N_{12} to the mean square fluctuation, i.e., $N = N_{12}/N_{11}$. As the distance between the points is increased, the correlation coefficient decreases from its maximum value of unity and becomes small compared to unity at a correlation distance. In other words, the statistical dependence between the fluctuations disappears.

The wavenumber spectra of the random perturbation, λ', ρ' and μ' can be expressed in terms of wavenumber spectra of the measured scattered field (see appendix):

$$[\frac{\lambda'(K^{pp})}{\alpha_0^4} + \frac{\rho'(K^{pp})}{\alpha_0^2}(\hat{i}\cdot\hat{g}) + 2\frac{\mu'(K^{pp})}{\alpha_0^4}(\hat{i}\cdot\hat{g})^2]k_l^s k_j^g = -4\rho_0^2\gamma_g^\alpha\gamma_s^\alpha U_{lj}^{pp} e^{-i(\gamma_s^\alpha x_s+\gamma_g^\alpha x_g)} \quad (1.4)$$

$$[\frac{\rho'(K^{ps})}{\alpha_0\beta_0}|\hat{i}\times\hat{g}| + \frac{\mu'(K^{ps})}{\alpha_0^2\beta_0^2}|\hat{i}\times\hat{g}|(\hat{i}\cdot\hat{g})]k_l^s k_J^g = -4\rho_0^2\gamma_g^\alpha\gamma_s^\beta U_{lj}^{ps} e^{-i(\gamma_s^\alpha x_s+\gamma_g^\beta x_g)} \quad (1.5)$$

$$[\frac{\rho'(K^{ps})}{\alpha_0\beta_0}|\hat{i}\times\hat{g}| + \frac{\mu'(K^{ps})}{\alpha_0^2\beta_0^2}|\hat{i}\times\hat{g}|(\hat{i}\cdot\hat{g}]k_L^s k_j^g = 4\rho_0^2\gamma_g^\beta\gamma_s^\alpha U_{lj}^{sp} e^{-i(\gamma_s^\beta x_s+\gamma_g^\alpha x_g)} \quad (1.6)$$

$$[\frac{\rho'(K^{ss})}{\beta_0^2}(\hat{i}\cdot\hat{g}) + \frac{\mu'(K^{ss})}{\beta_0^2}[(\hat{i}\cdot\hat{g})^2 - |\hat{i}\times\hat{g}|]k_l^s k_j^g = -4\rho_0^2\gamma_g^\beta\gamma_s^\beta U_{lj}^{ss} e^{-i(\gamma_s^\beta x_s+\gamma_g^\beta x_g)} \quad (1.7)$$

where

$$K^{pp} = k^\alpha\hat{g} - k^\alpha\hat{i}, \qquad K^{ps} = k^\beta\hat{g} - k^\alpha\hat{i},$$
$$K^{sp} = k^\alpha\hat{g} - k^\beta\hat{i}, \qquad K^{ss} = k^\beta\hat{g} - k^\beta\hat{i}.$$

These Equation (1.4 - 1.7) indicate the spectrum relation between the medium parameters and the observed scattered field of four different modes. Notice that

$$\begin{aligned}\hat{i}\cdot\hat{g} &= 1 - (\hat{g}-\hat{i})^2/2 = 1 - |K|^2/2k^2,\\ |\hat{i}\times\hat{g}| &= \frac{|K|}{k}\sqrt{1-|K|^2/4k^2}.\end{aligned}$$

These operators represent the coverage related to the observation geometry and the polarization.

We define the power spectrum as the Fourier transform of the auto-correlation or

cross-correlation. The auto-spectra or cross-spectra of the fluctuation of the elastic parameters is related to the power spectrum of the scattered fields, i.e.,

$$< m^*_{pp} m_{pp} >= (4\rho_0^2 \gamma_g^\alpha \gamma_s^\alpha)^2 < u'^{pp*}_{lj} u'^{pp}_{lj} > \tag{1.8}$$

$$< m^*_{ps} m_{ps} >= (4\rho_0^2 \gamma_g^\alpha \gamma_s^\beta)^2 < u'^{ps*}_{lj} u'^{ps}_{lj} > \tag{1.9}$$

$$< m^*_{sp} m_{sp} >= (4\rho_0^2 \gamma_g^\beta \gamma_s^\alpha)^2 < u'^{sp*}_{lj} u'^{sp}_{lj} > \tag{1.10}$$

$$< m^*_{ss} m_{ss} >= (4\rho_0^2 \gamma_g^\beta \gamma_s^\beta)^2 < u'^{ss*}_{lj} u'^{ss}_{lj} > \tag{1.11}$$

In Equation (1.8 to 1.11), the random functions characterize the medium by means of function $< m^*_{lj} m_{lj} >$. The product $< m^*_{lj} m_{lj} >$ is combination of the auto-correlation and cross-correlation spectra of the parameters of the random medium. For instance,

$$\begin{aligned} < m^*_{ps} m_{ps} >= & \frac{< \rho' \rho'^* >}{(\alpha_0 \beta_0)^2} |\hat{i} \times \hat{g}|^2 + 2\frac{< \rho' \mu'^* >}{(\alpha_0 \beta_0)^3} |\hat{i} \times \hat{g}|^2 (\hat{i} \cdot \hat{g}) \\ & + 2\frac{< \mu' \rho'^* >}{(\alpha_0 \beta_0)^3} |\hat{i} \times \hat{g}|^2 (\hat{i} \cdot \hat{g}) + 4\frac{< \mu' \mu'^* >}{(\alpha_0 \beta_0)^3} |\hat{i} \times \hat{g}|^2 (\hat{i} \cdot \hat{g})^2 \end{aligned} \tag{1.12}$$

Considering the fracture characterization, we assume $\rho' = 0$, then we have

$$< m^*_{ps} m_{ps} >= 4\frac{< \mu' \mu'^* >}{(\alpha_0 \beta_0)^3} |\hat{i} \times \hat{g}|^2 (\hat{i} \cdot \hat{g})^2 \tag{1.13}$$

NUMERICAL EXPERIMENTS

In this section we illustrate the theory discussed above with some numerical examples. We use finite difference and born approximation to simulate wave propagation in the random media, which are the realizations simulated with various correlation functions. Some of the issues of the modeling are discussed. Then we apply the diffraction tomographic inversion to the power spectrum of the scattered field to invert the correlation function (second moment) of the media. We also apply the method to Mcroly field data.

Simulation

First we study wave propagation using finite-difference. The observation system consisting of one shot and multiple receivers in a transmission geometry. The random models are (1) the realization simulated using Gaussian correlation function and (2) the realization simulated using exponential correlation function. The possible errors includes that result from finite grid size, finite simulation dimensions. In the implementation, we make sure that the first two statistical moments are correct. To satisfy the condition of stability and dispersion required in finite difference solver, the limits to p-wave velocity and s-wave velocity variations are imposed. These limits are large enough so that statistical parameters do not change.

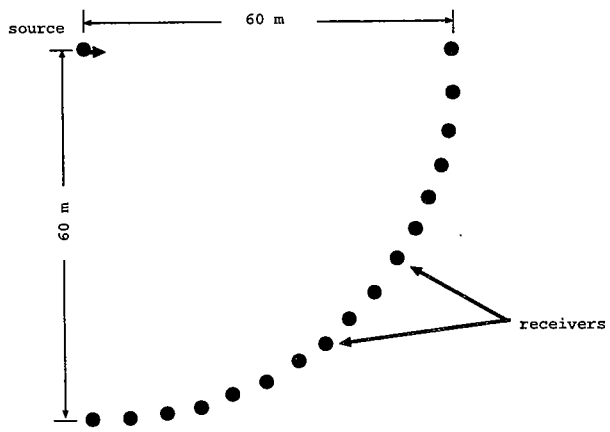

Figure 1.3: The geometry for calculate wave field with finite difference

In Figure 1.3, we show the geometry of the calculation. The receivers are placed at the positions have equal distance to the source location. The source is polarized in x direction. This geometry is easier to observe first arrive and radiation pattern. The simulation results are shown in Figure 1.4 and 1.4. We can see that although the first arrives are not sensitive to the inhomogeneities, the scattering is energetic and rich.

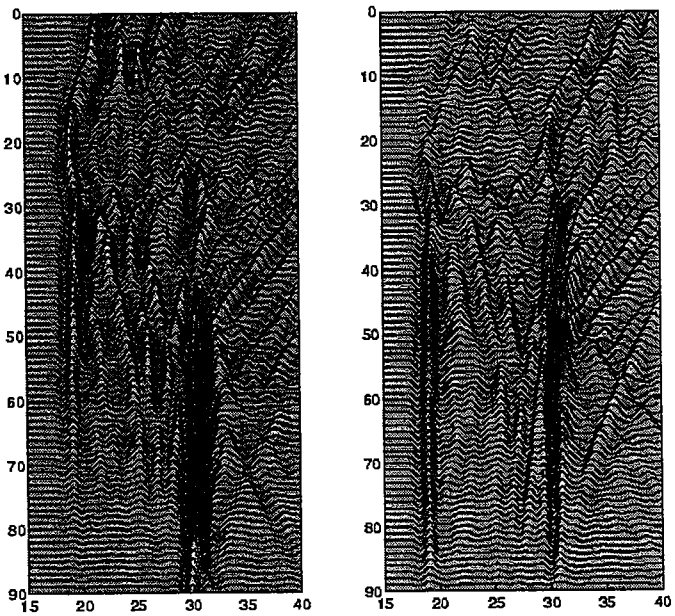

Figure 1.4: The finite difference simulation of the wave propagation in a exponential medium. The left panel is x-component and the right panel is z-component.

Synthetic example of inversion

Figure (1.6) shows the spatial distribution function, shared by ρ', μ', and λ'. The horizontal and vertical autocorrelation length is 12.5 and $1.25m$ respectively. This model may corresponded to oriented fractured rock. The corresponding p-wave velocity is $3500m/s$, s-wave velocity is $2121m/s$ and density is $2.6g/cm^3$. The wave length for the p-wave is $10m$ and the crosswell near offset is 20 λ.

In Figure 1.7 we show the spectrum of the field calculated according to Born approximation 1.4 - 1.7, described in appendix.

In Figure 1.8, we show the inverted correlation function of the medium. We can see that the retrieved correlation function match the model very well for horizontal and 45^o and 135^o orientations. At 90^o, the retrieved correlation function is severe distorted compared to the original model. The reasons are that cross well has the poorer resolution for vertical striper and a limited aperture is used both for generating data and inversion.

If the deviation of λ, μ and ρ form their average values are not small, the scattered

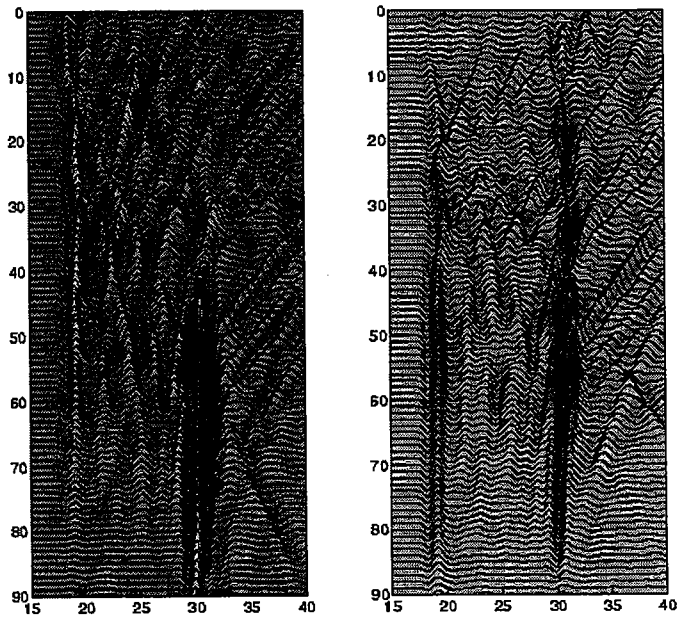

Figure 1.5: The finite difference simulation of the wave propagation in a Gaussian medium. The left panel is x-component and the right panel is z-component.

field will be small only if the region in which these deviations occur is small. This is the situation of thin scatterer which are considered as elements of fractures.

Inversion of field data

For the real data, we eliminated the first s-arrive and earlier arrives. We also perform 2.5D correction and normalize the amplitude (Harris et al. 1996). From a receiver gather of the McElroy near offset data set which is shown in Figure 6. We can see that there are many chaotic ss reflection/scattering features in the seismogram.

In Figure 1.10, we show the temporal power spectra of the processed data set at two distinct frequencies.

We invert the power spectra and get an autocorrelation function using diffraction tomographic technique discussed above. From Figure 8, we can see that the auto correlation obtained is strongly "anisotropic", i.e., the horizontal and vertical correlation lengths are quite different. This is expected since the other studies suggest the geology structure at the McElroy set are basically one dimensional. Note that

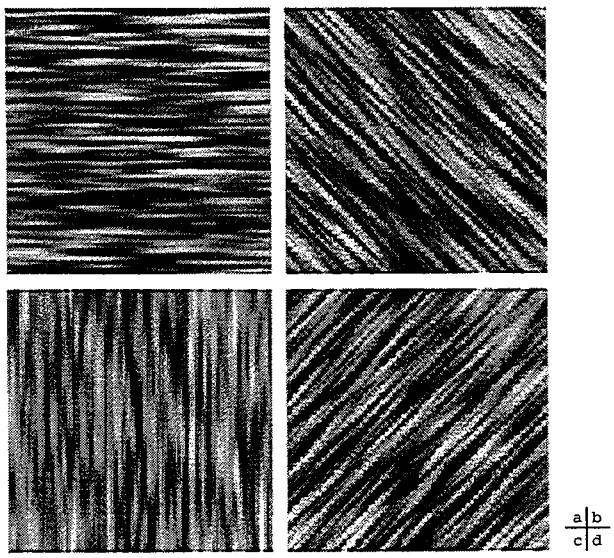

Figure 1.6: The correlation functions of the model. (a), (b), (c) and (d) corresponding to fractures are oriented in 0, 45, 90 and 135 degree respectively.

the correlation function is, in general, not of a particular elastic parameters but of a m_{ss} function described in Equation (1.11). If we assume $\rho' = 0$, then the correlation function is about the perturbation of the elastic constant μ'. It is possible to invert the correlation function of a particular perturbation of the elastic constant (Paper R of this report).

The power spectra of the processed wave field at two distinct frequencies: (a) and (b) are the spectrum at 1100 Hz and 1200 Hz, respectively.

CONCLUSIONS

The method discussed in this paper is an extension of the diffraction tomography. The resolved statistical quantities, such as the auto-correlation and cross-correlation of the random medium can be indirectly to characterize the porosity or permeability of the medium or facilitate other reservoir simulation modalities. For the perturbation theory discussed above to be applicable it is necessary that the scattering medium is statistically homogeneous which is a strong restriction in practical applications. The future research is to allow statistically inhomogeneous media as we do to diffraction

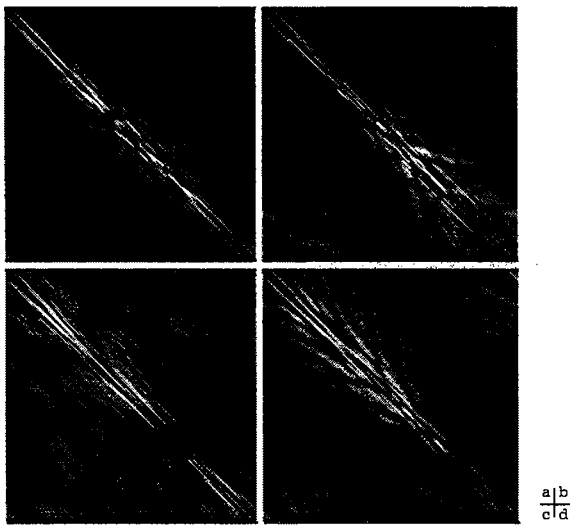

Figure 1.7: The spectral calculated according to Equation 1.7

tomography in general.

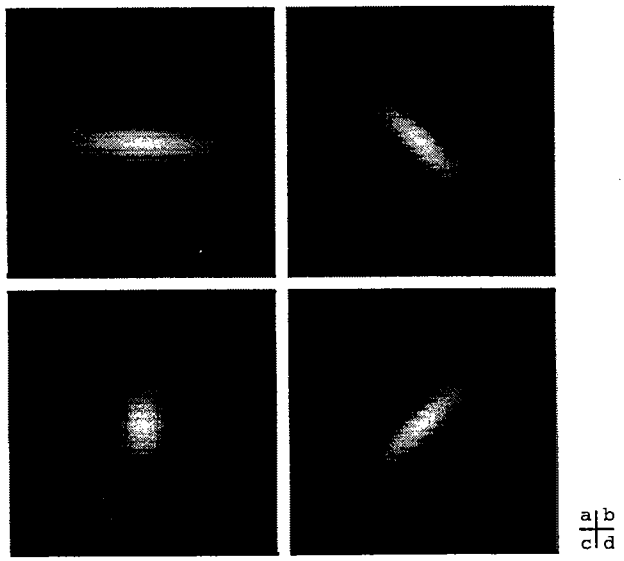

Figure 1.8: Inverted correlation functions. (a), (b), (c) and (d) corresponding to fractures are oriented in 0, 45, 90 and 135 degree respectively.

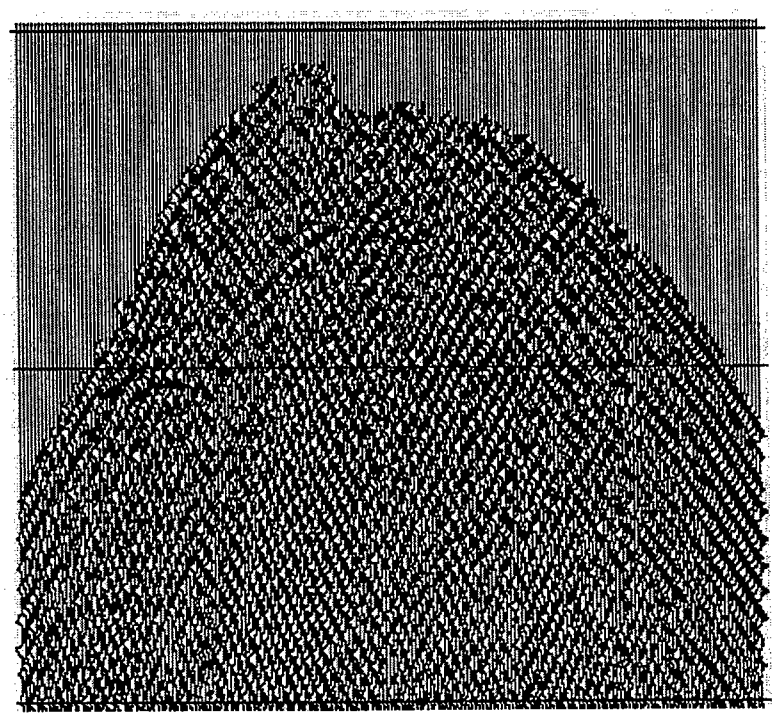

Figure 1.9: The wave field from McElroy near-offset data set. The first s-arrival has been eliminated.

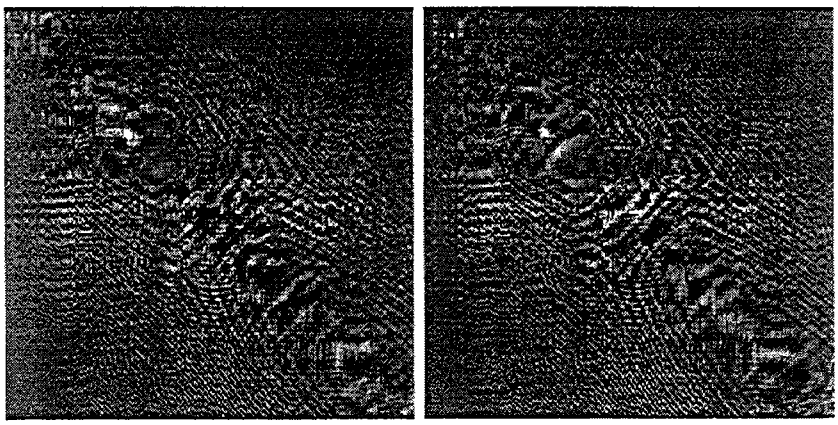

Figure 1.10: The power spectra of the processed wave field at two distinct frequencies: (a) and (b) are the spectrum at 1100 Hz and 1200 Hz, respectively.

Figure 1.11: Tomographic inversion of the random medium: (a) The spatial auto-power spectrum of the processed wave field of McElroy near-offset data set; and (b) Inverted autocorrelation function of the m_{ss} function.

REFERENCE

Aki, K., and Richards, P.G., 1980, Quantitative Seismology, vol. I: First edition, Freeman and Company, 273–286.

Harris, M. J., 1994, Lecture notes on random medium and scattering

Harris, M. J. and Guan Y. Wang, 1996, Diffraction tomography for inhomogeneities in layered background medium

Ikelle, L.T. and Yung, S.K., 1993, 2D random media with ellipsoidal autocorrelation functions: Geophysics (Sept. 1993) vol.58, no.9, p. 1359-72.

Muller, G., et al. "Seismic-wave traveltimes in random media." Geophysical journal international (July 1992) vol.110, no.1, p. 29-41.

Papoulis,A., 1984, Probability, random variables, and stochastic process. 2nd ed. New York: McGraw-Hill

APPENDIX

GREEN'S FUNCTION AND SINGLE SCATTERING OF ELASTIC MEDIA

The scattered field in a elastic medium can be written as (Aki and Richards, 1980)

$$U_{lj}(\mathbf{x}_s, \mathbf{x}_g, \omega) = -\int \{\omega^2 \rho' \tilde{G}_{li} \hat{G}_{ij} + \lambda' \tilde{G}_{lk,k} \hat{G}_{ij,i} + \mu' (\tilde{G}_{li,k} + \tilde{G}_{lk,i}) \hat{G}_{ij,k}\} d\mathbf{x}\,. \quad \text{(P.14)}$$

where $\tilde{G}_{ij} = G_{ij}(\mathbf{x}, \mathbf{x}_s)$ and $\hat{G}_{ij} = G_{ij}(\mathbf{x}_g, \mathbf{x})$ are Green's functions for source and receiver respectively. The displacement for a source in the l-direction and measurements in the j-direction can be represented as superposition of four wave types, i.e., P-to-P, P-to-S, S-to-P and S-to-S. Therefore

$$U_{lj} = U_{lj}^{pp} + U_{lj}^{ps} + U_{lj}^{sp} + U_{lj}^{ss}\,. \quad \text{(P.15)}$$

The two-dimensional Green's function for a homogeneous background is discussed in (reference ?) Appendix A. Here we give the results in the transform domain. For SH wave fields

$$G_{yy}(\mathbf{x}, k_s) = \frac{i}{2\mu_0 \gamma_s} e^{i(\gamma_s x_s - k \hat{s} \cdot \mathbf{x})} \quad \text{(P.16)}$$

For P-SV waves

$$\underset{\sim}{\mathbf{G}}(r, k_s) = \frac{i}{2\rho_0 \omega^2} \begin{vmatrix} (k_x^s)^2 & k_z^{\alpha s} K_x^s \\ k_z^{\alpha s} K_x^s & (k_z^{\alpha s})^2 \end{vmatrix} \frac{e^{i(\gamma_s^\alpha x_s - k^\alpha \hat{s} \cdot \mathbf{x})}}{\gamma_s^\alpha}$$

$$+ \frac{i}{2\rho_0 \omega^2} \begin{vmatrix} (k_z^{\beta s})^2 & -k_z^{\beta s} K_x^s \\ -k_z^{\beta s} K_x^s & (k_x^s)^2 \end{vmatrix} \frac{e^{i(\gamma_s^\beta x_s - k^\beta \hat{s} \cdot \mathbf{x})}}{\gamma_s^\beta} \quad \text{(P.17)}$$

Using Green's functions in (P.16) and (P.17) and apply single scattering approximation, one can obtain the Fourier wavenumber domain spectra of the scattered field (transformed along the source array and receiver array respectively).

$$U_{lj}^{pp}(k_s, k_g, \omega) = \frac{-1}{4\rho_0^2} \int [\frac{\lambda'}{\alpha_0^4} + \frac{\rho'}{\alpha_0^2} (\hat{i} \cdot \hat{g}) + \frac{2\mu'}{\alpha_0^2} (\hat{i} \cdot \hat{g})^2] k_l^s k_j^g S^p R^p d^2 r \quad \text{(P.18)}$$

$$U_{lj}^{ps}(k_s, k_g, \omega) = \frac{-1}{4\rho_0^2} \int [\frac{\rho'}{\alpha_0 \beta_0} |\hat{i} \times \hat{g}| + \frac{2\mu'}{\alpha_0^2 \beta_0^2} |\hat{i} \times \hat{g}| (\hat{i} \cdot \hat{g})] k_l^s k_J^g S^p R^s d^2 r \quad \text{(P.19)}$$

$$U_{lj}^{sp}(k_s,k_g,\omega)=\frac{-1}{4\rho_0^2}\int[\frac{\rho'}{\alpha_0\beta_0}|\hat{i}\times\hat{g}|+\frac{2\mu'}{\alpha_0^2\beta_0^2}]|\hat{i}\times\hat{g}|(\hat{i}\cdot\hat{g})k_L^sk_j^gS^sR^pd^2r \qquad \text{(P.20)}$$

$$U_{lj}^{ss}(k_s,k_g,\omega)=\frac{-1}{4\rho_0^2}\int[\frac{\rho'}{\beta_0^2}(\hat{i}\cdot\hat{g})+\frac{\mu'}{\beta_0^4}((\hat{i}\cdot\hat{g})^2-|\hat{i}\times\hat{g}|^2)]k_L^sk_J^gS^sR^sd^2r \qquad \text{(P.21)}$$

where

$$S^p=\frac{e^{i(\gamma_s^\alpha x_s-k^\alpha\hat{i}\cdot\mathbf{x})}}{\gamma_s^\alpha},\qquad S^s=\frac{e^{i(\gamma_s^\beta x_s-k^\beta\hat{i}\cdot\mathbf{x})}}{\gamma_s^\beta},$$
$$R^p=\frac{e^{i(\gamma_g^\alpha x_g-k^\alpha\hat{g}\cdot\mathbf{x})}}{\gamma_g^\alpha},\qquad R^s=\frac{e^{i(\gamma_g^\beta x_g-k^\beta\hat{g}\cdot\mathbf{x})}}{\gamma_g^\beta}.$$

In P.19-P.21, for the P-to-S and S-to-P modes,$k_J=k_L=k_z$ for $j=l=x$ and $k_J=k_L=-k_x$ for $j=l=z$. The convention for capital indexes given above holds for the S-to-S mode. Notice that

$$\hat{i}\cdot\hat{g}=1-(\hat{g}-\hat{i})^2/2=1-|K|^2/2k^2,$$
$$|\hat{i}\times\hat{g}|=\frac{|K|}{k}\sqrt{1-|K|^2/4k^2}.$$

These operators represent the coverage related to the observation geometry and the polarization.